Letter

Interacting triplons in frustrated spin ladders: Binding and decay in $BiCu_2PO_6$

Leanna B. Müller and Götz S. Uhrig *

Condensed Matter Theory, TU Dortmund University, Otto-Hahn-Straße 4, 44227 Dortmund, Germany

(Received 31 October 2022; revised 16 January 2023; accepted 23 January 2023; published 3 February 2023)

Establishing a comprehensive model of the rich spin dynamics in $BiCu_2PO_6$ has been a challenge over the last decade. Inelastic neutron scattering experiments revealed that its elementary triplons are nondegenerate, showing the existence of significant anisotropic spin couplings. Evidence for triplon decay into two triplons has been found, but two prominent downturns in the dispersions eluded an explanation. Level repulsion due to hybridization of single triplons with the continuum of two-triplon scattering states has been proposed as an explanation. We show that this concept may explain the weak downturn at higher energies, but fails for the most pronounced downturn at lower energy. In turn, we provide evidence that this downturn is the signature of a two-triplon bound state of essentially singlet character pointing to a triplon-triplon interaction as the second crucial ingredient of the spin dynamics in this exemplary system.

DOI: 10.1103/PhysRevB.107.L081102

Introduction. Strongly correlated quantum systems are notoriously difficult to understand due to the extremely fast growth of dimensionality of the relevant Hilbert space with system size. At low energies close to the ground state, however, the situation is much more favorable. Elementary excitations can be identified in terms of which most physical properties can be explained; they can be addressed as particles or quasiparticles of the system. For translationally invariant systems, i.e., in crystals, the dispersion $\hbar\omega(\vec{k})$ yields the energy dependence on the momentum $\hbar\vec{k}$ of the quasiparticles. Theoretically, this is described by a diagonal Hamiltonian which is bilinear in creation and annihilation operators. In addition, these excitations can decay, for instance, one excitation into two excitations which is captured by trilinear terms in the Hamiltonian. The pairwise interaction of two particles, called a two-particle interaction, is described by quadrilinear terms. Terms and processes involving even more quasiparticles may also arise and can be denoted by quintilinear terms and sextilinear terms (three-particle interactions) and so on. These higher interactions are rarely considered, but they do occur in effective models and can lead to important shifts of spectral weight and even bound states [1].

Here, we focus on systems formed by localized spins in insulators, so called quantum magnets. They provide clean and well-defined systems which are only weakly coupled to other degrees of freedom such as charges or phonons. Thus, the elementary excitations are long lived unless they decay intrinsically due to terms beyond the bilinear ones. Omnipresent pairwise interactions can lead to bound states. Hence, quasiparticle decay and binding are the two foci of the present Letter which we discuss in the particular system $BiCu_2PO_6$ realizing weakly coupled spin ladders [2].

There are three large classes of elementary excitations of quantum magnets. In systems with long-range magnetic order the elementary excitations are quantized spin waves, so called magnons. In low-dimensional or very strongly correlated systems fractional excitations occur called spinons. In gapped quantum antiferromagnets without order the elementary excitations above the $S = 0$ ground state have a triplet character with $S = 1$ and are called triplons [3] to underline their quasiparticle nature. For $BiCu_2PO_6$, these triplons are the relevant elementary excitations [4–7].

Theoretically, quasiparticle decay and its preconditions have been discussed generally [8,9] and for magnetic excitations in particular [10–14]. Experimentally, it has been observed in a number of ordered quantum magnets [15–17] and disordered quantum magnets [5,18,19] underlining the relevance of this issue. The decay of magnons is particularly strong if a single magnon can decay into two magnons as it is the case for noncollinear ordering, for instance, in triangular quantum antiferromagnets [14,16,20–23]. A noteworthy observation is that the trilinear terms also imply a renormalization of the energy of the single magnon by level repulsion. For large enough trilinear terms the dispersion is pushed below the multiparticle continuum so that decay no longer occurs; this has been dubbed "avoided quasiparticle decay" [14]. Generically, it is also seen in one-dimensional systems [11,12,14]. Similarly, decay processes from one quasiparticle to three quasiparticles also lead to a renormalization of the dispersion due to level repulsion as seen in the collinear square lattice Heisenberg antiferromagnet [24–26].

Binding stems from the quadrilinear terms as explained above. In quantum ferromagnets the fully polarized state is the ground state and the number of magnons is conserved in the model as given. Long ago, bound states of magnons in ferromagnets were established [27–30] and play a role in current applications [31]. For quantum antiferromagnets, the situation has more facets depending on the nature of the ground state. For unfrustrated antiferromagnets with long-range order, bound states of two magnons appear in gapped, easy-axis systems [26,32–34] which disappear on

*goetz.uhrig@tu-dortmund.de

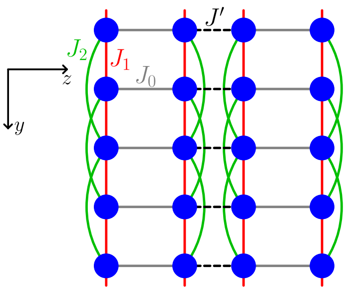

D^{α}_{ij}	along legs	parity
D^{y}_{0}	alternating	odd
D^{x}_{1}	uniform	odd
D^{y}_{1}	alternating	odd
D^{x}_{2}	uniform	odd
D^{z}_{2}	alternating	even

FIG. 1. Left: Sketch of the spin model for $BiCu_2PO_6$; blue spheres denote the Cu^{2+} ions hosting the spins $S = 1/2$. The isotropic couplings J_0, J_1, and J_2 define a single frustrated ladder while the isotropic interladder coupling J' weakly links adjacent ladders forming planes. Right: Sign of nonvanishing DM terms along the legs, parity with respect to reflection. The parity given for D^y_0 refers to its term in the Hamiltonian, not to D^y_0 itself.

passing to the isotropic antiferromagnet. But there remains a strong attractive force which shifts the spectral weight to lower energies and induces a rotonlike minimum in the magnon dispersion by level repulsion [24,25].

In one dimension, no long-range order occurs without spin anisotropies in the Hamiltonian. But fractional spinon excitations are established [35] which also form bound states [27,36,37]. They could be experimentally verified only recently [38]. We point out that triplon excitations can be also seen as bound states of confined spinons [39,40].

Gapped antiferromagnets with neither long-range order nor fractionalization are valence bond solids and their elementary excitations are triplons which generically attract each other, in particular if the total spin remains zero. This has been established for spin ladders [41–47], dimerized spin chains [48–51], and for the Shastry-Sutherland lattice [52–54], both in theory and experiment.

The compound. In this Letter, we elucidate the possibility of quasiparticle decay and binding in the strongly frustrated spin ladders in $BiCu_2PO_6$. The crystal structure has been discussed by Tsirlin *et al.* [2], but for our purposes the spin model is sufficient. The spins $S = 1/2$ are localized at the copper ions which are positioned in tubes made from an upper and a lower spin ladder. In addition, the spin ladders are weakly coupled forming a two-dimensional lattice [55,56]. Here, only the topology of the magnetic exchange couplings matters so that we project the upper and lower spin ladders in one plane (see Fig. 1).

The isotropic part of the Hamiltonian of a single frustrated spin ladder reads

$$\mathcal{H}_{\text{lad}} = J_0 \sum_i \mathbf{S}^{\text{L}}_i \mathbf{S}^{\text{R}}_i + J_1 \sum_{i,\tau} \mathbf{S}^{\tau}_i \mathbf{S}^{\tau}_{i+1} + J_2 \sum_{i,\tau} \mathbf{S}^{\tau}_i \mathbf{S}^{\tau}_{i+2}, \quad (1)$$

with the rung index i and the $\tau \in \{\text{L}, \text{R}\}$ indicating the left or right leg, respectively. The interladder coupling J' is significantly weaker than the intraladder couplings, but not negligible [2,4]. $BiCu_2PO_6$ represents a valence bond solid with triplons as elementary magnetic excitations because its spin system is gapped. Since the inversion symmetry about the Cu-Cu bonds is broken, anisotropic Dzyaloshinskii-Moriya (DM) couplings may occur [57] and were conjectured [2]. The splitting of the otherwise degenerate triplons [4,5] clearly confirms this conjecture.

Including anisotropic couplings to our model of $BiCu_2PO_6$ we discuss the Hamiltonian

$$\mathcal{H} = \mathcal{H}_{\text{lad}} + \sum_{i,j} \mathbf{D}_{ij}(\mathbf{S}_i \times \mathbf{S}_j) + \sum_{i,j} \sum_{\alpha,\beta} \Gamma^{\alpha\beta}_{ij} S^{\alpha}_i S^{\beta}_j. \quad (2)$$

Note that we include the label {L, R} indicating the leg of the ladder in the site indices i and j henceforth. In addition to $\mathcal{H}_{\text{lad}}$ from Eq. (1) we consider the DM interactions $\mathbf{D}_{ij}(\mathbf{S}_i \times \mathbf{S}_j)$ and the symmetric anisotropic exchanges $\Gamma^{\alpha\beta}_{ij} S^{\alpha}_i S^{\beta}_j$. The sums with the site indices i and j are meant to count each pair of spins once. The couplings along the rungs of the spin ladder are labeled with the index 0, thus J_0, $\mathbf{D}_0$, and $\Gamma^{\alpha\beta}_0$. The index 1 is used for all couplings between other nearest-neighbor (NN) sites, thus J_1, $\mathbf{D}_1$, and $\Gamma^{\alpha\beta}_1$. Lastly, the couplings between next-nearest-neighbor (NNN) sites are marked with the index 2, thus J_2, $\mathbf{D}_2$, and $\Gamma^{\alpha\beta}_2$; see also Fig. 1. The symmetric anisotropic exchanges $\Gamma^{\alpha\beta}_{ij}$ represent the second-order effects of the DM terms [58] reading

$$\Gamma^{\alpha}_{ij} = \frac{D^{\alpha}_{ij} D^{\beta}_{ij}}{2J_{ij}} - \frac{\delta^{\alpha\beta} \mathbf{D}_{ij}}{6J_{ij}}, \quad (3)$$

and being defined such that the tensor Γ_{ij} is traceless [6]. The orientation of the $\mathbf{D}$ vectors is determined by the selection rules based on the point group symmetries [57] (see Fig. 1). The symmetry analysis [6] yields the results displayed on the right-hand side of Fig. 1. Five DM components can assume finite values from which four components hold odd parity with respect to reflection about the center line of the spin ladder [46]. Hence they do not contribute to bilinear terms in the Hamiltonian, but only to trilinear and potential quintilinear terms.

Theoretical analyses. The approach used extends the treatment in Ref. [6] in two steps. Step (i) starts from the isolated isotropic spin ladder which we map by a continuous unitary transformation (CUT) [59,60] to an effective model formulated in second quantization, i.e., in creation and annihilation operators of the elementary excitations, triplons [3,40,61]. In this step, we take the hardcore property of the triplons fully into account. This effective model conserves the number of triplons so that the computation of physical properties such as the dispersion, bound states, or spectral densities is greatly facilitated.

The CUT represents a systematic basis change and can be applied as well to any observable, in particular to the spin components $S_{i,\alpha}$. In step (ii), we use these transformed observables to express all residual couplings [antisymmetric ($\propto \mathbf{D}_{ij}$) and symmetric DM terms ($\propto \Gamma^{\alpha\beta}_{i,j}$), interladder couplings ($\propto J'$)] in terms of triplon operators. In order to cope with these additional bilinear and trilinear terms we treat the triplons appearing in them as usual bosons without hardcore property, for instance, the bilinear terms can be diagonalized by a Bogoliubov transformation. This is justified in this second step because of the smallness of the additional couplings. The quadrilinear terms are taken from the CUT in step (i) of the isolated ladders and also subjected to the Bogoliubov transformation. In view of the three momenta which can be varied freely in quadrilinear terms with momentum

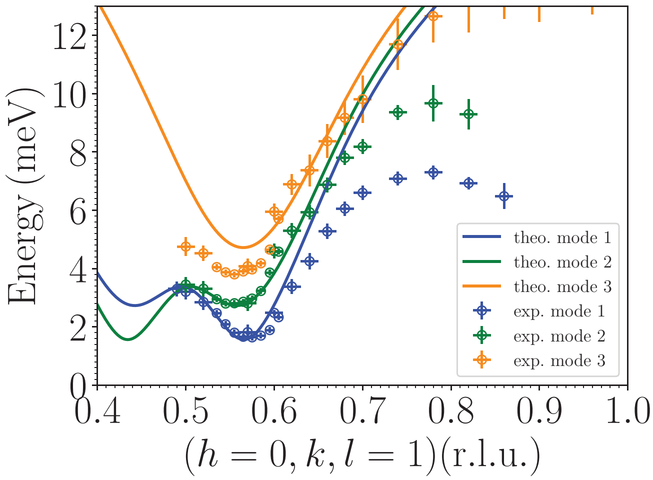

FIG. 2. Energies in the bilinear model for $BiCu_2PO_6$ for the parameters $J_0 = 9.4$ meV, $J_1 = 1.2J_0$, $J_2 = 0.9J_1$, $J' = 1.5$ meV, $D_0^y = 0$, $D_1^x = 0.48J_1$, $D_1^y = 0.61J_1$, $D_2^x = 0$, and $D_2^z = -0.02J_2$. Unlinked symbols are the experimental data from Refs. [5,62].

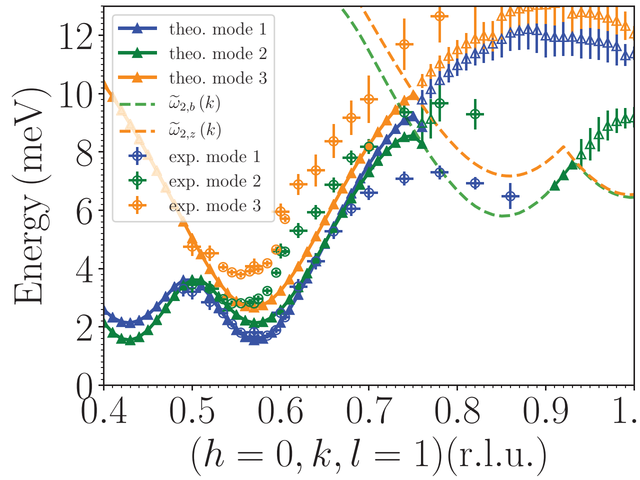

FIG. 3. Dispersion in the trilinear model. Energetically low-lying dispersion including the hybridization between the one- and the two-triplon states. A weak down-bending occurs before the single triplon dispersion enters the two-triplon continua at about $k = 0.75$ r.l.u. The parameters used are $J_0 = 8.0$ meV, $J_1 = 1.2J_0$, $J_2 = 0.9J_1$, $J' = 0.16J_0$, $D_0^y = 0.1J_0$, $D_1^x = 0.25J_1$, $D_1^y = 0.38J_1$, $D_2^x = 0.0$, and $D_2^z = -0.09J_2$. The dashed lines represent the lower edges of the two-triplon continua. The yellow curve is computed from the highest yellow dispersion, and the green one from the green dispersion. All other four continua edges lie between the two depicted continuum edges. Unlinked open circles are the experimental data from Refs. [5,62]. The unlinked open triangles indicate resonances within the two-triplon continuum and the vertical bars show their half width at half maximum (HWHM) being proportional to the decay rate.

conservation, this comprises a particularly large number of coefficients representing the numerical bottleneck in this calculation. From the resulting terms we keep the two-triplon interaction terms consisting of monomials of two creation and two annihilation operators. They are responsible for the binding phenomena.

Finally, we compute resolvents in the hybridized one-triplon and two-triplon subspace at a given total momentum $\hbar\mathbf{q}$. These resolvents provide access to the dynamic structure factor $S(\mathbf{q}, \omega)$ including sharp resonances outside the continuum of scattering states (see the Appendix). The momentum dependence of these sharp resonances is to be compared with the dispersion of the experimentally observed strong peaks. Sharp resonances can stem from either single triplon states which are renormalized by the hybridization with the two-triplon states or from bound two-triplon states.

Bilinear level. Previously, we performed the analysis of experimental inelastic neutron scattering (INS) data for $BiCu_2PO_6$ on the bilinear level and achieved best fits with the parameters given in the caption of Fig. 2; for details, see Ref. [6]. The dispersions in the vicinity of the minima are captured very well except for the shift of the upper mode. But the downturns of the measured data remain completely unexplained. Additionally, the values of the NN DM terms are substantially larger than one is expecting for the relative strength of couplings stemming from spin-orbit coupling: 10%–20% of the corresponding exchange coupling. Qualitatively, these findings agree with those by Hwang and Kim [7] for the bilinear model.

Trilinear level. This brings us to the trilinear terms resulting from the DM couplings of odd parity which introduce a new piece of physics, namely the decay of a triplon into two triplons and vice versa the fusion of two triplons to a single one so that the one- and the two-triplon subspaces hybridize. The results are shown in Fig. 3. The dispersion minima are captured in their position in k space, but their energy splitting is underestimated so that the bilinear model fits the dispersion minima better. This is due to the much more demanding numerical evaluation on the trilinear level which does not allow us to scan all conceivable parameter combinations, for instance, we stick to the ratios J_1/J_0 and J_2/J_1 determined on the bilinear level.

One satisfying observation underlining the importance of the trilinear terms is that the required DM couplings are much lower than on the bilinear level. The value for D_1^x has lowered from $0.48J_1$ to $0.25J_1$ and for D_1^y from $0.61J_1$ to $0.38J_1$ which brings them closer to the expected range of spin-orbit induced couplings. On the downside, however, we only find a weak feature of level repulsion in Fig. 3. There is a small downturn in the dispersions (green or blue) just before it enters into the scattering continuum at $k \approx 0.75$ reciprocal lattice units (r.l.u.) and $\hbar\omega \approx 9$ meV. Comparing this feature to the significant experimental downturn (blue symbols) beginning at $k = 0.7$ r.l.u. at around 7 meV, it is evident that the hybridization due to trilinear terms is insufficient to explain the measured features. This conclusion agrees with the figures from previous calculations [7]. We deduce that the level repulsion between the single triplon states and the scattering two-triplon states forming the continuum alone is too weak to account for the observed dispersions. This raises the question about what generates the experimental features. Promising candidates are bound states since it is known that spin ladders host bound two-triplon states [41–47]. In addition, frustration enhances binding because the mobility of triplons is reduced while their interaction is enhanced [49–51].

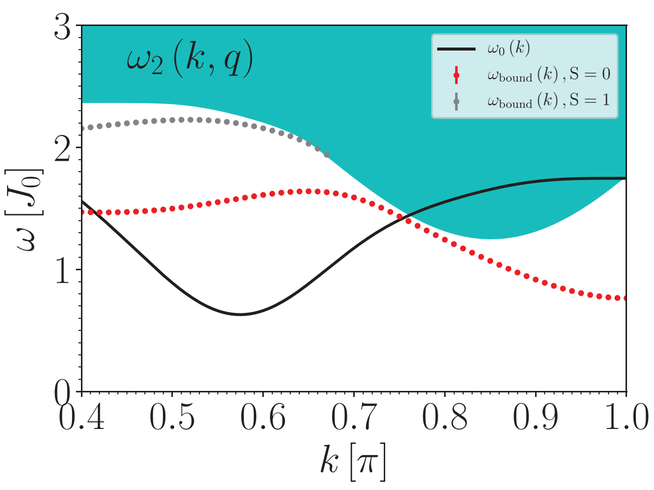

FIG. 4. Isolated spin ladder for $J_1 = 1.2J_0$, $J_2 = 0.9J_1$: The one-triplon dispersion in black, and two-triplon continuum is colored; the $S_{\rm tot} = 0$ bound state is shown by the dotted red line, and the $S_{\rm tot} = 1$ bound state by the dotted gray line. The wave number is given in units of π with a lattice constant of unity. This corresponds to the reciprocal lattice units of $BiCu_2PO_6$ where the lattice constant is the distance between next-nearest-neighbor rungs [2,6].

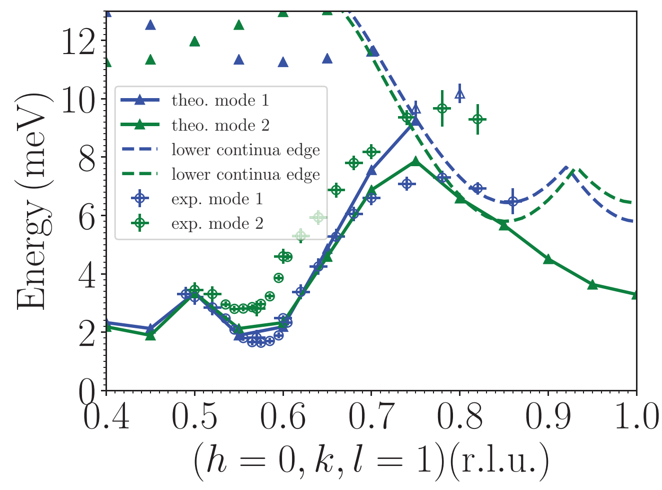

FIG. 5. Energies in the quadrilinear model for $BiCu_2PO_6$ for $J_0 = 8.0$ meV, $J_1 = 1.2J_0$, $J_2 = 0.9J_1$, $J' = 0.16J_0$, $D_0^y = 0.1J_0$, $D_1^x = 0.25J_1$, $D_1^y = 0.38J_1$, $D_2^x = 0.0$, and $D_2^z = -0.06J_2$. The green (blue) dashed line shows the lower continuum edge derived from the dispersion displayed as a green (blue) solid line. Unlinked open circles are the experimental data from Refs. [5,62]. The unlinked open triangles indicate resonances within the two-triplon continuum and the vertical bars show their HWHM being proportional to the decay rate.

Quadrilinear level. Describing the binding of two particles requires including the quadrilinear terms in second quantization. First, we inspect the isolated ladder for which the CUT alone yields the effective model very reliably. Figure 4 displays the dispersions of a single triplon and of the two bound states formed by two triplons. The latter are situated below the two-triplon band of scattering states shaded in light green-blue. It is remarkable that just at $k \approx 0.75$ r.l.u. the $S_{\rm tot} = 0$ state, displayed by the red dotted curve, falls below the single triplon dispersion. This suggests that a bound state could indeed be involved in the experimental situation. A counterargument is that INS is sensitive only to $S = 1$ states, not to $S = 0$ states. While this holds in spin isotropic systems it does not apply in the presence of the sizable spin anisotropies existing in $BiCu_2PO_6$. For completeness, we also depict the bound $S = 1$ state by the gray dotted curve.

As a next step, we compute the dynamic structure factor including the triplon-triplon interaction in the full two-dimensional (2D) model in reciprocal space with in the Hilbert space spanned by one-triplon and two-triplon states at a given total momentum. This is a very demanding calculation because the matrix representing the Hamiltonian is no longer sparse. In the previous trilinear case, the Hamiltonian relevant for the two-triplon subspace is diagonal. The triplon-triplon interaction, however, implies scattering between the states of all relative momenta so that the corresponding matrix is dense. We performed calculations for 40×8 **k** points. The results are shown in Fig. 5. Clearly, an additional branch with significant weight forks off the dispersion of the single dispersion at $k \approx 0.75$ r.l.u. with ≈ 7 meV. This agrees very well with the most prominent downturn in experiment. It provides evidence that two-triplon interactions and the concomitant binding are essential players in the physics of $BiCu_2PO_6$. The bound state is not observed in experiment at 1 r.l.u. because it is an $S_{\rm tot} = 0$ state and visible only due to the DM terms. Beyond 0.8 r.l.u. its weight becomes very small [63].

Unfortunately, the resolution of the present calculation is not high enough for a tangible statement about the second downturn (green circles) at about $k = 0.75$ r.l.u. at ≈ 9 meV. It could result from a weaker bound state formed from triplons of different flavors. Note that the spin anisotropies split the triplons and hybridize them so that they acquire mixed flavors. An alternative and appealing explanation for the second downturn is suggested by the results for the trilinear model (see Fig. 3). While they do not explain the strong downturn at about 7 meV, they may explain the weak downturn around 9 meV due to level repulsion [5]. The wave vector and the energy at which this downturn occurs agree between theory and experiment as well as the overall size of the feature. These observations call for future high-precision calculations including trilinear *and* quadrilinear terms. In this way, the intricate interplay between hybridization and the attractive interaction in $BiCu_2PO_6$ can be elucidated quantitatively. The lesson learned will provide the foundation for understanding many more strongly frustrated low-dimensional quantum antiferromagnets where tri- and quadrilinear processes need to be measured and understood.

Similarly to the trilinear model, the quadrilinear model does not capture the low-lying dispersions very well because it underestimates the splitting between the blue and the green mode. Again, this can be attributed to the fact that no parameter fit was possible on the quadrilinear level due to the very resource-intensive calculations. We essentially used the parameters of the trilinear model.

Conclusion. Summarizing, we analyzed the unusual dispersions found in $BiCu_2PO_6$ with respect to two important phenomena: decay and binding. Decay results from trilinear terms in second quantization formed by two creation and one annihilation operator or their Hermitian conjugate representing fusion. Binding stems from quadrilinear terms formed by two creation and two annihilation operators. Generically, both types are present and their importance relative to the single-particle dispersion is particularly high in low-dimensional systems. $BiCu_2PO_6$ is a challenging exemplary system to study these fundamental processes because it hosts significant spin anisotropy terms so that different triplon flavors can be distinguished by their energy. In this system, evidence for the relevance of trilinear terms was found [5,7]. Yet the strong, dominant downturn eluded an explanation. Our analysis including a triplon-triplon interaction, i.e., with quadrilinear terms, suggests that the strong downturn is the signature of an $S = 0$ two-triplon bound state, slightly perturbed by the anisotropic terms so that it becomes visible in the dynamic structure factor measured by inelastic neutron scattering. The weak downturn at higher energies can be identified as the signature of level repulsion between a single triplon and the two-triplon scattering continuum. These findings suggest $BiCu_2PO_6$ as a challenging exemplary platform to investigate the phenomena of the binding and decay of multiflavor quasiparticles.

Acknowledgments. This study was funded by the German Research Foundation (DFG) in Grant No. UH 90/14-1. Parts of the calculations were performed on the LiDO3 high-performance computing system funded by the DFG. We acknowledge useful discussions with Nils Drescher; he also provided the code to perform the CUT. We thank Carsten Nase for lasting technical support.

APPENDIX: TECHNICAL DETAILS

The dynamic structure factor in the time domain reads

$$S^{\alpha\beta}(\mathbf{q},\omega) = \frac{1}{2\pi}\int_{-\infty}^{\infty} dt\, e^{i\omega t}\langle S^{\alpha}(-\mathbf{q},t)S^{\beta}(\mathbf{q},0)\rangle. \tag{A1}$$

At zero temperature, its Fourier transform for $\alpha = \beta$ is given by the retarded Green's function

$$G^{\mathrm{ret},\alpha}(\mathbf{q},\omega) = \langle u_0|\frac{1}{\omega - H(\mathbf{q})}|u_0\rangle, \tag{A2}$$

where $|u_0\rangle = S^{\alpha}(\mathbf{q},0)|0\rangle$ with $|0\rangle$ being the ground state. We omit α henceforth since we focus on the energies and not on the spectral weights here.

The action of the Hamiltonian in (A2) is represented by a tridiagonal matrix,

$$\bar{H}(\mathbf{q}) = \begin{pmatrix} a_0(\mathbf{q}) & b_1(\mathbf{q}) & 0 & 0 & \cdots \\ b_1(\mathbf{q}) & a_1(\mathbf{q}) & b_2(\mathbf{q}) & 0 & \cdots \\ 0 & b_2(\mathbf{q}) & a_3(\mathbf{q}) & b_3(\mathbf{q}) & \cdots \\ \vdots & \vdots & \vdots & \vdots & \ddots, \end{pmatrix}, \tag{A3}$$

which is computed by a Lanczos iteration,

$$|u_1\rangle = [H(\mathbf{q}) - a_0(\mathbf{q})]|u_0\rangle, \tag{A4a}$$

$$|u_2\rangle = [H(\mathbf{q}) - a_1(\mathbf{q})]|u_1\rangle - b_1^2(\mathbf{q})|u_0\rangle, \tag{A4b}$$

$$|u_3\rangle = [H(\mathbf{q}) - a_2(\mathbf{q})]|u_2\rangle - b_2^2(\mathbf{q})|u_1\rangle,$$
$$\ldots, \tag{A4c}$$

yielding the coefficients

$$a_i(\mathbf{q}) = \frac{\langle u_i|H(\mathbf{q})|u_i\rangle}{\langle u_i|u_i\rangle} \quad \text{for } i = 0, 1, 2, \ldots, \tag{A5a}$$

$$b_i^2(\mathbf{q}) = \frac{\langle u_i|u_i\rangle}{\langle u_{i-1}|u_{i-1}\rangle} \quad \text{for } i = 1, 2, 3, \ldots, \tag{A5b}$$

$$b_0(\mathbf{q}) = 0. \tag{A5c}$$

Finally, the Green's function is computed by its continued fraction down to a certain depth of 30–100 fractions,

$$G^{\mathrm{ret}}(\mathbf{q},\omega) = \cfrac{1}{\omega - a_0(\mathbf{q}) - \cfrac{b_1^2(\mathbf{q})}{\omega - a_1(\mathbf{q}) - \cfrac{b_2^2(\mathbf{q})}{\omega - a_2(\mathbf{q}) - \cdots}}}. \tag{A6}$$

Then, the continued fraction is terminated by the square root terminator,

$$T(\mathbf{q},\omega) = \frac{1}{2b_\infty^2(\mathbf{q})}[\omega - a_\infty(\mathbf{q}) - \sqrt{R(\mathbf{q},\omega)}] \tag{A7a}$$

$$\text{for } \omega \geqslant \omega_{2,\max}(\mathbf{q}), \tag{A7b}$$

$$T(\mathbf{q},\omega) = \frac{1}{2b_\infty^2(\mathbf{q})}[\omega - a_\infty(\mathbf{q}) - i\sqrt{-R(\mathbf{q},\omega)}]$$
$$\text{for } \omega_{2,\min} \leqslant \omega \leqslant \omega_{2,\max}(\mathbf{q}),$$

$$T(\mathbf{q},\omega) = \frac{1}{2b_\infty^2(\mathbf{q})}[\omega - a_\infty(\mathbf{q}) + \sqrt{R(\mathbf{q},\omega)}]$$
$$\text{for } \omega \leqslant \omega_{2,\min}(\mathbf{q}), \tag{A7c}$$

where we used

$$\omega_{2,\min}(\mathbf{q}) = a_\infty(\mathbf{q}) - 2b_\infty(\mathbf{q}), \tag{A8a}$$

$$\omega_{2,\max}(\mathbf{q}) = a_\infty(\mathbf{q}) + 2b_\infty(\mathbf{q}), \tag{A8b}$$

and

$$R(\mathbf{q},\omega) = [\omega - a_\infty(\mathbf{q})]^2 - 4b_\infty^2(\mathbf{q}). \tag{A9}$$

[1] G. Schmiedinghoff, L. Müller, G. S. Uhrig, U. Kumar, and B. Fauseweh, Three-body bound states in antiferromagnetic spin ladders, Commun. Phys. **5**, 218 (2022).

[2] A. A. Tsirlin, I. Rousochatzakis, D. Kasinathan, O. Janson, R. Nath, F. Weickert, C. Geibel, A. M. Läuchli, and H. Rosner, Bridging frustrated-spin-chain and spin-ladder physics: Quasi-one-dimensional magnetism of $BiCu_2PO_6$, Phys. Rev. B **82**, 144426 (2010).

[3] K. P. Schmidt and G. S. Uhrig, Excitations in One-Dimensional $S = 1/2$ Quantum Antiferromagnets, Phys. Rev. Lett. **90**, 227204 (2003).

[4] K. W. Plumb, Z. Yamani, M. Matsuda, G. J. Shu, B. Koteswararao, F. C. Chou, and Y.-J. Kim, Incommensurate

dynamic correlations in the quasi-two-dimensional spin liquid $BiCu_2PO_6$, Phys. Rev. B **88**, 024402 (2013).
[5] K. W. Plumb, K. Hwang, Y. Qiu, L. W. Harriger, G. E. Granroth, A. I. Kolesnikov, G. J. Shu, F. C. Chou, C. Rüegg, Y. B. Kim, and Y.-J. Kim, Quasiparticle-continuum level repulsion in a quantum magnet, Nat. Phys. **12**, 224 (2016).
[6] L. Splinter, N. A. Drescher, H. Krull, and G. S. Uhrig, Minimal model for the frustrated spin ladder system $BiCu_2PO_6$, Phys. Rev. B **94**, 155115 (2016).
[7] K. Hwang and Y. B. Kim, Theory of triplon dynamics in the quantum magnet $BiCu_2PO_6$, Phys. Rev. B **93**, 235130 (2016).
[8] L. P. Pitaevski, Properties of the spectrum of elementary excitations near the disintegration threshold of the excitations, Sov. Phys. JETP **36**, 830 (1959).
[9] B. Gaveau and L. S. Schulman, Limited quantum decay, J. Phys. A **28**, 7359 (1995).
[10] M. E. Zhitomirsky, Decay of quasiparticles in quantum spin liquids, Phys. Rev. B **73**, 100404(R) (2006).
[11] T. Fischer, S. Duffe, and G. S. Uhrig, Adapted continuous unitary transformation to treat systems with quasi-particles of finite lifetime, New J. Phys. **12**, 033048 (2010).
[12] T. Fischer, Description of quasiparticle decay by continuous unitary transformations, Ph.D. thesis, TU Dortmund University, 2011.
[13] M. E. Zhitomirsky and A. L. Chernyshev, Spontaneous magnon decays, Rev. Mod. Phys. **85**, 219 (2013).
[14] R. Verresen, R. Moessner, and F. Pollmann, Avoided quasiparticle decay from strong quantum interactions, Nat. Phys. **15**, 750 (2019).
[15] T. Hong, M. Matsumoto, Y. Qiu, W. Chen, T. R. Gentile, S. Watson, F. F. Awwadi, M. M. Turnbull, S. E. Dissanayake, H. Agrawal, R. Toft-Petersen, B. Klemke, K. Coester, K. P. Schmidt, and D. A. Tennant, Field-induced spontaneous quasiparticle decay and renormalization of quasiparticle dispersion in a quantum antiferromagnet, Nat. Commun. **8**, 15148 (2017).
[16] J. Oh, M. D. Le, J. Jeong, J.-H. Lee, H. Woo, W.-Y. Song, T. G. Perring, W. J. L. Buyers, S.-W. Cheong, and J.-G. Park, Magnon Breakdown in a Two Dimensional Triangular Lattice Heisenberg Antiferromagnet of Multiferroic $LuMnO_3$, Phys. Rev. Lett. **111**, 257202 (2013).
[17] N. J. Robinson, F. H. L. Essler, I. Cabrera, and R. Coldea, Quasiparticle breakdown in the quasi-one-dimensional Ising ferromagnet $CoNb_2O_6$, Phys. Rev. B **90**, 174406 (2014).
[18] M. B. Stone, I. A. Zaliznyak, T. Hong, C. L. Broholm, and D. H. Reich, Quasiparticle breakdown in a quantum spin liquid, Nature (London) **440**, 187 (2006).
[19] T. Masuda, A. Zheludev, H. Manaka, L.-P. Regnault, J.-H. Chung, and Y. Qiu, Dynamics of Composite Haldane Spin Chains in IPA-$CuCl_3$, Phys. Rev. Lett. **96**, 047210 (2006).
[20] W. Zheng, J. O. Fjærestad, R. R. P. Singh, R. H. McKenzie, and R. Coldea, Excitation spectra of the spin-$\frac{1}{2}$ triangular-lattice Heisenberg antiferromagnet, Phys. Rev. B **74**, 224420 (2006).
[21] A. L. Chernyshev and M. E. Zhitomirsky, Spin waves in a triangular lattice antiferromagnet: Decays, spectrum renormalization, and singularities, Phys. Rev. B **79**, 144416 (2009).
[22] M. Mourigal, W. T. Fuhrman, A. L. Chernyshev, and M. E. Zhitomirsky, Dynamical structure factor of the triangular-lattice antiferromagnet, Phys. Rev. B **88**, 094407 (2013).
[23] M. Mourigal, W. T. Fuhrman, A. L. Chernyshev, and M. E. Zhitomirsky, Erratum: Dynamical structure factor of the triangular-lattice antiferromagnet, Phys. Rev. B **93**, 099901(E) (2016).
[24] M. Powalski, G. S. Uhrig, and K. P. Schmidt, Roton Minimum as a Fingerprint of Magnon-Higgs Scattering in Ordered Quantum Antiferromagnets, Phys. Rev. Lett. **115**, 207202 (2015).
[25] M. Powalski, K. P. Schmidt, and G. S. Uhrig, Mutually attracting spin waves in the square-lattice quantum antiferromagnet, SciPost Phys. **4**, 001 (2018).
[26] R. Verresen, F. Pollmann, and R. Moessner, Quantum dynamics of the square-lattice Heisenberg model, Phys. Rev. B **98**, 155102 (2018).
[27] H. Bethe, Zur Theorie der Metalle. I. Eigenwerte und Eigenfunktionen der linearen Atomkette, Z. Phys. **71**, 205 (1931).
[28] F. J. Dyson, General theory of spin-wave interactions, Phys. Rev. **102**, 1217 (1956).
[29] J. Hanus, Bound States in the Heisenberg Ferromagnet, Phys. Rev. Lett. **11**, 336 (1963).
[30] M. Wortis, Bound States of Two Spin Waves in the Heisenberg Ferromagnet, Phys. Rev. **132**, 85 (1963).
[31] J. Barker, U. Atxitia, T. A. Ostler, O. Hovorka, O. Chubykalo-Fesenko, and R. W. Chantrell, Two-magnon bound state causes ultrafast thermally induced magnetisation switching, Sci. Rep. **3**, 3262 (2013).
[32] T. Oguchi and T. Ishikawa, Theory of two-magnon bound states in a two-dimensional antiferromagnet, J. Phys. Soc. Jpn. **34**, 1486 (1973).
[33] C. J. Hamer, Energy spectrum of the two-magnon bound states in the Heisenberg-Ising antiferromagnet on the square lattice, Phys. Rev. B **79**, 212413 (2009).
[34] S. Dusuel, M. Kamfor, K. P. Schmidt, R. Thomale, and J. Vidal, Bound states in two-dimensional spin systems near the Ising limit: A quantum finite-lattice study, Phys. Rev. B **81**, 064412 (2010).
[35] L. D. Faddeev and L. A. Takhtajan, What is the spin of a spin wave? Phys. Lett. A **85**, 375 (1981).
[36] M. Kohno, Dynamically Dominant Excitations of String Solutions in the Spin-1/2 Antiferromagnetic Heisenberg Chain in a Magnetic Field, Phys. Rev. Lett. **102**, 037203 (2009).
[37] M. Ganahl, E. Rabel, F. H. L. Essler, and H. G. Evertz, Observation of Complex Bound States in the Spin-1/2 Heisenberg XXZ Chain Using Local Quantum Quenches, Phys. Rev. Lett. **108**, 077206 (2012).
[38] Z. Wang, J. Wu, W. Yang, A. K. Bera, D. Kamenskyi, A. T. M. N. Islam, S. Xu, J. M. Law, B. Lake, C. Wu, and A. Loidl, Experimental observation of Bethe strings, Nature (London) **554**, 219 (2018).
[39] M. Greiter, Two-leg t-J ladder: A spin liquid generated by Gutzwiller projection of magnetic bands, Phys. Rev. B **65**, 134443 (2002).
[40] M. Kohno, O. A. Starykh, and L. Balents, Spinons and triplons in spatially anisotropic frustrated antiferromagnets, Nat. Phys. **3**, 790 (2007).
[41] D. G. Shelton, A. A. Nersesyan, and A. M. Tsvelik, Antiferromagnetic spin ladders: Crossover between spin $S = 1/2$ and $S = 1$ chains, Phys. Rev. B **53**, 8521 (1996).
[42] O. P. Sushkov and V. N. Kotov, Bound States of Magnons in the $S = 1/2$ Quantum Spin Ladder, Phys. Rev. Lett. **81**, 1941 (1998).

[43] S. Trebst, H. Monien, C. J. Hamer, Z. Weihong, and R. R. P. Singh, Strong-Coupling Expansions for Multiparticle Excitations: Continuum and Bound States, Phys. Rev. Lett. **85**, 4373 (2000).

[44] C. Knetter, K. P. Schmidt, M. Grüninger, and G. S. Uhrig, Fractional and Integer excitations in Quantum Antiferromagnetic Spin $1/2$ Ladders, Phys. Rev. Lett. **87**, 167204 (2001).

[45] M. Windt, M. Grüninger, T. Nunner, C. Knetter, K. P. Schmidt, G. S. Uhrig, T. Kopp, A. Freimuth, U. Ammerahl, B. Büchner, and A. Revcolevschi, Observation of Two-Magnon Bound States in the Two-Leg Ladders of $(Ca,La)_{14}Cu_{24}O_{41}$, Phys. Rev. Lett. **87**, 127002 (2001).

[46] K. P. Schmidt and G. S. Uhrig, Spectral properties of magnetic excitations in cuprate two-leg ladder systems, Mod. Phys. Lett. B **19**, 1179 (2005).

[47] S. Notbohm, P. Ribeiro, B. Lake, D. A. Tennant, K. P. Schmidt, G. S. Uhrig, C. Hess, R. Klingeler, G. Behr, B. Büchner, M. Reehuis, R. I. Bewley, C. D. Frost, P. Manuel, and R. S. Eccleston, One- and Two-Triplon Spectra of a Cuprate Ladder, Phys. Rev. Lett. **98**, 027403 (2007).

[48] A. M. Tsvelik, Spectrum of magnetic excitations in the spin-Peierls state, Phys. Rev. B **45**, 486 (1992).

[49] G. S. Uhrig and H. J. Schulz, Magnetic excitations spectrum of dimerized antiferromagnetic chains, Phys. Rev. B **54**, R9624 (1996).

[50] G. S. Uhrig and H. J. Schulz, Erratum: Magnetic excitation spectrum of dimerized antiferromagnetic chains [Phys. Rev. B **54**, R9624 (1996)], Phys. Rev. B **58**, 2900(E) (1998).

[51] K. P. Schmidt, C. Knetter, and G. S. Uhrig, Spectral properties of the dimerized and frustrated $S = 1/2$ chain, Phys. Rev. B **69**, 104417 (2004).

[52] C. Knetter, A. Bühler, E. Müller-Hartmann, and G. S. Uhrig, Dispersion and Symmetry of Bound States in the Shastry-Sutherland Model, Phys. Rev. Lett. **85**, 3958 (2000).

[53] P. Lemmens, M. Grove, M. Fischer, G. Güntherodt, V. N. Kotov, H. Kageyama, K. Onizuka, and Y. Ueda, Collective Singlet Excitations and Evolution of Raman Spectral Weights in the 2D Spin Dimer Compound $SrCu_2(BO_3)_2$, Phys. Rev. Lett. **85**, 2605 (2000).

[54] C. Knetter and G. S. Uhrig, Dynamic Structure Factor of the Two-Dimensional Shastry-Sutherland Model, Phys. Rev. Lett. **92**, 027204 (2004).

[55] O. Mentré, E. M. Ketatni, M. Colmont, M. Huve, F. Abraham, and V. Petricek, Structural features of the modulated $BiCu_2(P_{1-x}V_x)O_6$ solid solution; 4-D treatment of $x = 0.87$ compound and magnetic spin-gap to gapless transition in new Cu^{2+} two-leg ladder systems, J. Am. Chem. Soc. **128**, 10857 (2006).

[56] S. Wang, E. Pomjakushina, T. Shiroka, G. Deng, N. Nikseresht, C. Rüegg, H. M. Rønnow, and K. Conder, Crystal growth and characterization of the dilutable frustrated spin-ladder compound $Bi(Cu_{1-x}Zn_x)_2PO_6$, J. Cryst. Growth **313**, 51 (2010).

[57] T. Moriya, Anisotropic superexchange interaction and weak ferromagnetism, Phys. Rev. **120**, 91 (1960).

[58] L. Shekhtman, O. Entin-Wohlman, and A. Aharony, Moriya's anisotropic superexchange interaction, frustration, and Dzyaloshinsky's weak ferromagnetism, Phys. Rev. Lett. **69**, 836 (1992).

[59] C. Knetter and G. S. Uhrig, Perturbation theory by flow equations: dimerized and frustrated $S = 1/2$ chain, Eur. Phys. J. B **13**, 209 (2000).

[60] H. Krull, N. A. Drescher, and G. S. Uhrig, Enhanced perturbative continuous unitary transformations, Phys. Rev. B **86**, 125113 (2012).

[61] S. Sachdev, Quantum magnetism and criticality, Nat. Phys. **4**, 173 (2008).

[62] K. W. Plumb, K. Hwang, Y. Qiu, L. W. Harriger, G. E. Granroth, G. J. Shu, F. C. Chou, Ch. Ruegg, Y. B. Kim, and Y.-J. Kim, Giant anisotropic interactions in the copper based quantum magnet $BiCu_2PO_6$, arXiv:1408.2528v1.

[63] L. B. Müller, Quasiparticle decay induced by spin anisotropies in the frustrated spin ladder system $BiCu_2PO_6$, Ph.D. thesis, TU Dortmund University, 2021.